

Journal of Photonics for Energy

SPIEDigitalLibrary.org/jpe

Solution processed hybrid photovoltaics: preparation of a standard ZnO template

Jonathan Downing
Mary P. Ryan
Natalie Stingelin
Martyn A. McLachlan

Solution processed hybrid photovoltaics: preparation of a standard ZnO template

Jonathan Downing, Mary P. Ryan, Natalie Stingelin,
and Martyn A. McLachlan

Imperial College London, Department of Materials and Centre for Plastic Electronics, London
Centre for Nanotechnology, London, SW7 2AZ, United Kingdom
martyn.mclachlan@imperial.ac.uk

Abstract. The formation of a well-defined, reproducible ZnO nanorod scaffold for hybrid photovoltaic applications has been investigated. A standard hydrothermal growth method was used and the influence of chemical additions in controlling length, width, density, and orientation was studied. The nanostructures prepared have been characterized by scanning electron microscopy, x-ray diffraction, UV-visible spectroscopy in addition to measurement of the wetting behavior. A standard procedure for the production of vertically orientated nanorods with a narrow size distribution, high areal density, and good wettability in aqueous solutions is presented. © 2011 Society of Photo-Optical Instrumentation Engineers (SPIE). [DOI: [10.1117/1.3569104](https://doi.org/10.1117/1.3569104)]

Keywords: solar energy; photovoltaic systems; sol-gels; microscopy.

Paper 10140SSPR received Aug. 15, 2010; revised manuscript received Feb. 20, 2011; accepted for publication Feb. 28, 2011; published online Mar. 22, 2011.

1 Introduction

The development of hybrid (inorganic:organic) photovoltaic devices (h-PV) is an attractive prospect because of the suitability of such devices for low-cost solution processing. However, wide-spread use is still limited by two significant challenges; conversion efficiency and cost.¹ In this paper a simple method is outlined for the preparation of well-defined nanostructured ZnO scaffolds that can be used to improve device efficiency. In principle, an organic component, e.g., a conjugated polymer with controlled morphology, electrical and absorption properties, combined with an appropriate inorganic semiconductor, e.g., ZnO, in which structure, transport, and surface properties can be readily tuned, should provide dramatic improvements over organic photovoltaics (OPV) devices. However, to date h-PV devices have demonstrated low conversion efficiencies,^{2,3} normally attributed to the limited exciton diffusion length in conjugated polymers (5 to 10 nm).⁴ Charge separation occurs at the heterojunction between the ZnO (acceptor) and the polymer (donor), therefore the ideal structure can be envisaged as an interconnected-array in which exciton generation occurs in the vicinity of an interface.⁵ The intimate intermixing of donor-acceptor species can be achieved in a number of ways but an engineered heterojunction ensures direct pathways for the free charge carriers to the electrodes, ensuring that efficient transport and collection occurs. In h-PV devices the morphology control in the donor-acceptor composite may be achieved by first constructing the inorganic scaffold with the appropriate layout and dimensions.⁶ This combination of materials presents an exciting opportunity for the development of h-PV devices that can overcome the current challenges and realize performance improvement by controlling the morphology of the active layer, which is considered to be a crucial step necessary for the evolution of efficient h-PV devices.²

ZnO is attractive for use in photovoltaic devices as it offers a direct electron pathway, effective light-scattering centers,¹ is low cost, and can be formed in a wide variety of nanostructures

from solution. In addition to PV applications^{7–11} nanostructured ZnO has been widely used in a range of applications including light emitting diodes,^{12–14} thin film transistors,¹⁵ and as chemical sensors.^{16,17} Nanostructured materials offer significantly larger interfacial areas than bulk films, however the challenge of preparing nanostructures with tailored and well-defined structures with high surface-area-to-volume ratios that maximize light harvesting while being compatible with the short polymer exciton diffusion length has continued to be problematic. Although several publications detail the formation of h-PV devices based on ZnO nanorods, reported efficiencies remain modest compared with OPV devices.^{3,18,19} The formation of metal oxide nanorod scaffolds has led to performance improvements compared with planar devices.^{7,8,18} More recently it has been shown that blended ZnO:P3HT h-PV devices with efficiencies of 2% can be prepared,⁶ stimulating further h-PV research.

Clearly a dispersed nanorod array fulfills many of the requirements necessary to improve device performance. Indeed there have been numerous techniques investigated in an effort to achieve this goal, including; electrochemical deposition,^{20,21} template directed growth,²² pulsed laser deposition,²³ and hydrothermal methods.^{24–27} While solution-based methods tend to favor the formation of a large number of rods, control of their aspect ratio, spacing, and orientation has yet to be demonstrated. Vacuum-based methods show potential for morphological control but are inherently unsuitable for scale-up.

There is a requirement for the preparation of tailored ZnO structures, in which the rod dimensions, spacing and orientation can be controlled. Such structures would open up a pathway for further improving h-PV device performance through compatibility with exciton diffusion length, in addition to providing direct pathways to the electrodes to minimize carrier transport time and the probability of back electron transfer.¹⁹ In this paper a method for the reproducible preparation of ZnO nanorod arrays using entirely solution-based methods is discussed. In such arrays the rod aspect ratio can be tuned by varying the growth conditions resulting in uniform length and vertically aligned structures. More importantly, the rod spacing can also be controlled which allows structures to be prepared that are ideal for preparing tailored h-PV devices with controlled separation between donor-acceptor centers.

2 Experimental

ZnO nanorods were created via a two-step solution-based process. First, a seed layer of ZnO was deposited by spin-coating a 0.75 M solution of zinc acetate dihydrate [$\text{Zn}(\text{O}_2\text{CCH}_3)_2 \cdot 2(\text{H}_2\text{O})$, Sigma-Aldrich] and 2-Aminoethanol [$\text{H}_2\text{N}(\text{CH}_2)_2\text{OH}$, Sigma-Aldrich] in 2-methoxyethanol [$\text{HO}(\text{CH}_2)_2\text{OCH}_3$, Sigma-Aldrich]²⁸ onto indium tin oxide (ITO)-coated glass substrates (PsiOteC UK Ltd; 12 to 16 Ω/sq). A dense uniform layer was prepared by loading at 500 rpm and increasing the spin speed to 2000 rpm for 30 s. The process was repeated three times with the substrates briefly heated to 300°C between coats. A final 60 min anneal at 450°C was carried out after the layers had been deposited.

In the second step, the as-prepared substrates with ZnO seed layers were suspended upside down in an equimolar (25 mM) solution of HMT [$\text{NH}_2(\text{CH}_2)_6\text{NH}(\text{CH}_2)_6\text{NH}_2$, Sigma-Aldrich] and zinc nitrate [$\text{Zn}(\text{NO}_3)_2$, Sigma-Aldrich] at 95°C in a similar method described by Vayssieres.³⁰ The additives 10 mM polyethylenimine [$\text{H}(\text{NHCH}_2\text{CH}_2)_n\text{NH}_2$, Sigma-Aldrich] and/or 0.1 M potassium chloride (KCl, Sigma-Aldrich) were added directly to the solution. Following rod deposition the films were rinsed thoroughly with deionized water and allowed to dry at 95°C.

Scanning electron microscope (SEM) images were obtained using a Leo 1525 field emission scanning electron microscope. Cross-sectional images of the rod assemblies were obtained to determine rod length, by scratching or cleaving the substrate. Surface images were used to measure rod diameter. Data analysis was carried out using ImageJ software.

X-ray diffraction (XRD) patterns were obtained using a Panalytical X'Pert Pro diffractometer equipped with a monochromated Cu $K\alpha$ source and an accelerator detector. The voltage and current were set at 40 kV and 40 mA, respectively.

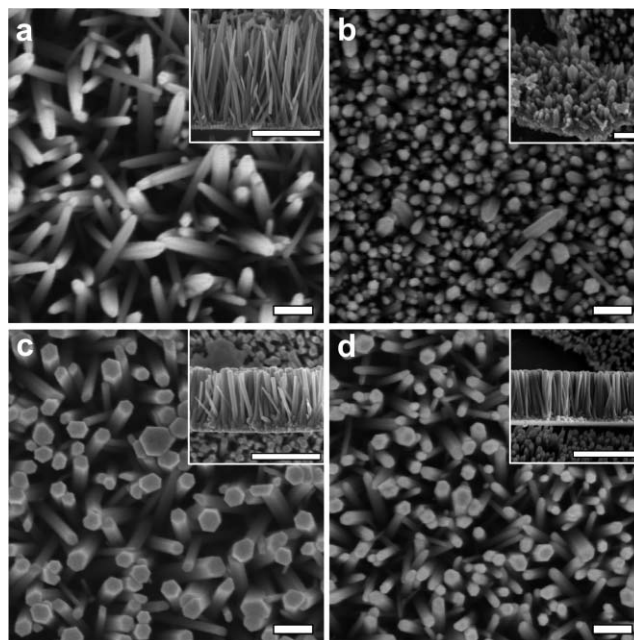


Fig. 1 SEM micrographs showing top-surface rod morphology and cleaved cross sections (insets) for ZnO rods grown by hydrothermal method under the conditions, (a) additive free growth, (b) addition of PEI (10 mM), (c) addition of KCl (100 mM), and (d) combined addition of PEI (10 mM) and KCl (100 mM). Main scale markers 200 nm, inset 500 nm.

3 Results and Discussion

3.1 Seed Layer Growth

Thin ZnO seed layers have been deposited onto ITO substrates by spin-coating a mixed precursor solution. The method has been adapted to lower the annealing temperature (450°C versus 600°C). Differential scanning calorimetry measurements carried out on the zinc acetate precursor show two distinct regions of mass loss on heating and a sharp crystallization peak at ~250°C on cooling. The technique results in the formation of polycrystalline thin films, confirmed by SEM (Fig. 1) and XRD (Fig. 2). Variations in chemical bath conditions and seed layer morphology have been shown to control rod density, diameter, and morphology.^{25,27,29}

3.2 Nanorod Growth

Rod formation occurs due to preferential growth of ZnO in the $\langle 001 \rangle$ direction. This can be explained by considering the structure of the unit cell. The hexagonal lattice consists of two networks of tetragonally coordinated Zn and O atoms, this coordination gives rise to polar asymmetry along the, $\langle 001 \rangle$ direction. Nanorod formation is described by Ashford et al.²⁴ for hydrothermal growth, whereby the high temperature decomposition of hexamethylene triamine (HMT) results in hydroxyl ion formation. OH^- anions produced in the vicinity of the polar ZnO surfaces are able to react with Zn^{2+} to produce the insoluble and thermodynamically unstable $\text{Zn}(\text{OH})_2$ species. The spontaneous decomposition of $\text{Zn}(\text{OH})_2$ results in the formation of ZnO, and growth continues at the polar surface resulting in the formation of rod structures. Nucleation of rod growth occurs on the ZnO seed layer and the structure of the rods is closely related to the morphology of the seed layer.

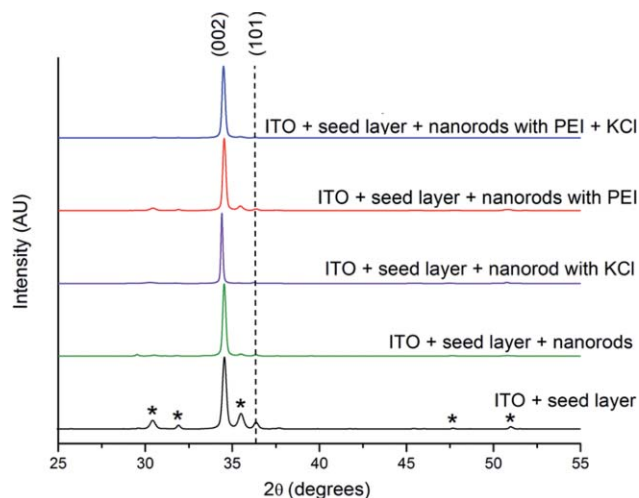


Fig. 2 X-ray diffraction patterns obtained from ZnO seed layers and nanorod arrays, curves labelled from bottom to top; seed layer on ITO (* indicates peaks from ITO substrate), additive-free nanorod growth, addition of PEI (10 mM), addition of KCl (100 mM), and combined addition of PEI (10 mM) and KCl (100 mM).

In this work nanorod arrays have been formed from various hydrothermal growth solutions. The seed layers used were prepared under identical conditions on glass-coated ITO substrates. First, the method outlined by Vayssieres³⁰ was repeated and resulted in the formation of overlapping nanorods with a large variation in the rod length and width [Fig. 1(a)]. The role of a surfactant [polyethylenimine (PEI)] was then investigated, it has been reported that reduced lateral growth of the rods occurs on the addition of PEI.¹⁰ The structures typically formed consisted of short nanorods [Fig. 1(b)] that differ from those reported in the literature. We attribute the variation to differences in the morphology of the seed layers. In the next experiments KCl was added to the growth solution. It has been well-reported that addition of KCl to an electrochemical deposition bath results in the formation of more uniform nanorod structures.³¹ When it is added to the hydrothermal growth solution the nanorod arrays prepared show an improved alignment and the rod length is more uniform with a planar surface termination [Fig. 1(c)]. In the final series of experiments the addition of both PEI and KCl was investigated. The structures prepared consist of uniform length nanorods aligned perpendicular to the substrate [Fig. 1(d)]. The combination of the additives gives an increase in rod density that results in very closely spaced arrays.

For the first time KCl has been shown to play a major role in morphological control of ZnO nanorods formed by hydrothermal deposition. The addition of KCl is seen to increase rod nucleation, therefore reducing the spacing between rods, and improve orientation thus ensuring an open structure for subsequent polymer infiltration. The rods formed when KCl was added also show well-defined hexagonal facets and are terminated by a planar (002) surface, which is stabilized during growth by the addition of Cl^- .²⁹ PEI is known to hinder lateral growth by absorbing onto the nonpolar (101) planes.¹⁰ The SEM images show a clear variation in the rod length, width, and density. To assess this, images have been analyzed using ImageJ software to quantify the average rod length, width, and rod density — the results are summarized in Table 1. To ensure representative quantities of rods were analyzed, the diameter, length, and density of 250 rods in each sample set were measured. It was not possible to extract meaningful statistics for the rods formed with the addition of only PEI because of their non-ideal morphology and broad size distribution [Fig. 1(b)].

Table 1 Rod dimensions and areal density obtained on various nanorod films. Values in brackets display standard deviation.

	Average rod diameter (nm)	Average rod length (nm)	Areal density/ μm^2
ITO + seed layer + nanorods (bare)	78 (29)	1283 (387)	45
ITO + seed layer + nanorods with KCl	81 (27)	895 (161)	35
ITO + seed layer + nanorods with KCl and surfactant	51 (22)	836 (20)	86

3.3 Contact Angle Measurement

The uptake of the rod arrays as electron accepting layers in h-PV devices is reliant on the ability to form composite structures with semiconducting polymers. Ideally, efficient filling of the structures would be achieved by filling from solution, hence it is necessary to understand the wetting behavior of the structures prepared. This was investigated with water as a solvent. Briefly a 3 μl droplet was added to the surface of various films and the contact angle measured. Large values of measured contact angle are indicative of poor wetting. The results are summarized in Table 2.

There is a clear improvement in the wetting behavior with the inclusion of additives into the growth solution. Importantly, the reported superhydrophobic behavior documented in ZnO nanorod arrays^{32,33} is not observed in these structures.

3.4 X-Ray Diffraction

The formation of crystalline ZnO has been confirmed using x-ray diffraction (Fig. 2). The lower temperature route used in seed layer deposition results in the formation of polycrystalline thin films with a {002} preferential orientation, consistent with previous reports.^{25–27} All of the nanorod structures prepared show the same preferential orientation, which is consistent with the structures observed by SEM and the proposed growth model.

Analysis of the diffraction data to calculate crystallite size is shown in Table 3, where sizes for the (002) and (101) diffraction peaks are given. The crystallite sizes calculated from the (002) diffraction peaks all show an extremely large size (larger than the region for Scherrer analysis), as is apparent in the peak narrowing observed in the XRD patterns (Fig. 2). The addition of KCl results in the smallest grain size extracted from the (101) data but the largest out-of-plane grain size (002), as evidenced by the narrow peak in the XRD pattern. Addition of PEI and the KCl/PEI mixture led to small increases in the measured (101) crystallite size. The measured (101) sizes

Table 2 Measured contact angle (water) for substrate, seed layer, and ZnO nanorods.

Substrate	Contact angle (deg)
ITO	55
ITO + seed layer	51
ITO + seed layer + nanorods (bare)	15
ITO + seed layer + nanorods with PEI	34
ITO + seed layer + nanorods with KCl	7
ITO + seed layer + nanorods with PEI and KCl	6

Table 3 Calculated crystallite sizes for seed layer and nanorod films prepared under the conditions described. The addition of KCl is seen to significantly increase the intensity of the 002 diffraction peaks.

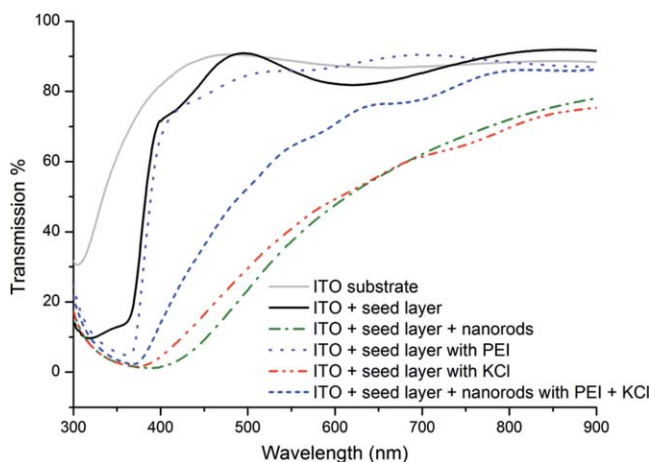
	Crystallite size (nm) $d_{(002)}$	Crystallite size (nm) $d_{(101)}$	002/101 Peak Intensity ^a
Seed layer	71	56	10
No additives	—	105	58
KCl	—	46	83
Surfactant	—	60	45
KCl and surfactant	—	70	141

^aIncludes contribution from seed-layer.

are similar to those measured for the seed layer, which confirms the role the seed layer has in controlling nanorod growth. For clarity, normalized (002) spectra are shown, however in the raw data the addition of KCl increases the intensity of the (002) diffraction peak relative to the (101) peak indicative of more orientated ZnO being deposited.

3.5 UV-Visible Spectroscopy

The optical transparency of the films was measured from 300 to 900 nm against an air background; the results are shown in Fig. 3. The ITO/glass substrate shows a strong absorption at <320 nm that rises sharply to give the substrate a transparency of >90% over the 400 to 900 nm range. The ZnO absorption band (360 nm) is apparent when the seed layer is added to the ITO and the transparency remains comparable to the bare substrate. The additive-free growth and the growth with PEI produce films that have significant scattering losses, which we attribute to the misalignment of the rods. The addition of KCl reduces the scattering and the KCl/PEI mixture produces a film with similar optical properties to only the seed layer. These films have fewer scattering losses owing to the morphology of the rods. The aligned structures are also beneficial for h-PV applications as they have more rods per unit area (increased interfacial area), and with less overlap between rods there are fewer obstacles to complete polymer infiltration.

**Fig. 3** UV-visible data for ITO substrate, seed layer, and nanorod arrays.

4 Conclusions

The development of a nanostructured ZnO template for h-PV applications is described. Hydrothermal growth has been identified as an appropriate method for the formation of nanorod arrays. Unmodified growth results in the formation of ZnO rods with a broad size distribution and a low density. Furthermore the rods are poorly aligned and overlapping. Orientated rods are necessary for h-PV applications; more rods per unit area increase interfacial area and matches closely with the exciton diffusion length in typical organic components. In addition, with less overlap between rods there are fewer obstacles to complete polymer infiltration, and voids are seen to be present when filling disordered ZnO structures.^{11,18}

To improve the quality of the rod arrays the influence of additives, PEI and KCl, to the hydrothermal growth bath was investigated. PEI is reported as an absorbent on the nonpolar faces of the growing ZnO nanorod while the role of KCl has until now been unreported. The addition of the surfactant results in the formation of short, tapered, and misaligned rods. The wetting behavior of the rods is nonideal and the UV-visible spectra show increased scattering. The addition of KCl significantly improves the uniformity of rod length and width and results in arrays composed of rods with improved alignment, and well-defined faceted rods are formed. The improvement in the wetting behavior of these arrays is attributed to the stabilization of the polar (002) surface at the tip of the rods. The combination of PEI and KCl addition results in ZnO arrays with the most desirable properties. Rods with a narrow size distribution and a high number density are prepared; additionally the rods are highly aligned and are terminated by (002) surfaces that gives rise to the improved wetting behavior. The highly aligned rods reduce scattering losses, which will be beneficial for h-PV devices, as it will ensure maximum photon density in the conjugated polymer.

Acknowledgments

Dr Benoit Illy and Joe Franklin for useful discussions. J.D. is supported by EPSRC DTA and in part by the Energy Futures Lab, Imperial College London. M.A.M. is grateful for the award of a Royal Academy of Engineering/EPSRC Research Fellowship.

References

1. Q. Zhang, C. S. Dandeneau, X. Zhou, and G. Cao, "ZnO Nanostructures for dye-sensitized solar cells," *Adv. Mater.* **21**(41), 4087–4108 (2009).
2. W. J. E. Beek, M. M. Wienk, M. Kemerink, X. N. Yang, and R. A. J. Janssen, "Hybrid zinc oxide conjugated polymer bulk heterojunction solar cells," *J. Phys. Chem. B.* **109**(19), 9505–9516 (2005).
3. D. C. Olson, J. Piris, R. T. Collins, S. E. Shaheen, and D. S. Ginley, "Hybrid photovoltaic devices of polymer and ZnO nanofiber composites," *Thin Solid Films* **496**(1), 26–29 (2006).
4. M. S. White, D. C. Olson, N. Kopidakis, A. M. Nardes, D. S. Ginley, and J. J. Berry, "Control of charge separation by electric field manipulation in polymer-oxide hybrid organic photovoltaic bilayer devices," *Phys. Status Solidi A* **207**(5), 1257–1265 (2010).
5. M. Helgesen, R. Sondergaard, and F. C. Krebs, "Advanced materials and processes for polymer solar cell devices," *J. Mater. Chem.* **20**(1), 36–60 (2010).
6. S. D. Oosterhout, M. M. Wienk, S. S. van Bavel, R. Thiedmann, L. Jan Anton Koster, J. Gilot, J. Loos, V. Schmidt, and R. A. J. Janssen, "The effect of three-dimensional morphology on the efficiency of hybrid polymer solar cells," *Nat. Mater.* **8**(10), 818–824 (2009).
7. D. C. Olson, S. E. Shaheen, R. T. Collins, and D. S. Ginley, "The effect of atmosphere and ZnO morphology on the performance of hybrid poly(3-hexylthiophene)/ZnO nanofiber photovoltaic devices," *J. Phys. Chem. C* **111**, 16670–16678 (2007).

8. D. Olson, Y.-J. Lee, M. S. White, N. Kopidakis, S. E. Shaheen, D. S. Ginley, J. A. Voigt, and J. W. P. Hsu, "Effect of ZnO Processing on the photovoltage of ZnO/Poly(3-hexylthiophene) solar cells," *J. Phys. Chem. C* **112**(26), 9544–9547 (2008).
9. P. Ravirajan, A. M. Peiro, M. K. Nazeeruddin, M. Graetzel, D. D. C. Bradley, J. R. Durrant, and J. Nelson, "Hybrid polymer/zinc oxide photovoltaic devices with vertically oriented ZnO nanorods and an amphiphilic molecular interface layer," *J. Phys. Chem. B* **110**(15), 7635–7639 (2006).
10. M. Law, L. E. Greene, J. Johnson, R. Saykally, and P. D. Yang, "Nanowire dye-sensitized solar cells," *Nat. Mater.* **4**(6), 455–459 (2005).
11. Y.-J. Lee, M. T. Lloyd, D. Olson, R. K. Grubbs, P. Lu, R. J. Davis, J. A. Voigt, and J. W. P. Hsu, "Optimization of ZnO nanorod array morphology for hybrid photovoltaic devices," *J. Phys. Chem. C* **113**(35), 15778–15782 (2009).
12. Y. Alivov, E. Kalinina, A. Cherenkov, and D. Look, "Fabrication and characterization of n-ZnO/p-AlGaIn heterojunction light-emitting diodes on 6H-SiC substrates," *Appl. Phys. Lett.* **83**(23), 4719–4721 (2003).
13. A. Osinsky, J. Dong, M. Kauser, and B. Hertog, "MgZnO/ AlGaIn heterostructure light-emitting diodes," *Appl. Phys. Lett.* **85**(19), 4272–4275 (2004).
14. Ü. Özgür, Y. Alivov, C. Liu, A. Teke, M. A. Reshchikov, S. Doğan, V. Avrutin, S.-J. Cho, and H. Morkoç, "A comprehensive review of ZnO materials and devices," *J. Appl. Phys.* **98**(4), 041301 (2005).
15. A. Bashir, P. H. Wöbkenberg, J. Smith, J. M. Ball, G. Adamopoulos, D. D. C. Bradley, and T. D. Anthopoulos, "High-performance zinc oxide transistors and circuits fabricated by spray pyrolysis in ambient atmosphere," *Adv. Mater.* **21**(21), 2226–2231 (2009).
16. O. Lupan, L. Chow, and G. Chai, "A single ZnO tetrapod-based sensor," *Sens. Actuators B* **141**(2), 511–517 (2009).
17. Y.-Z. Lv, C.-R. Li, L. Guo, F. Wang, Y. Xu, and X. Chu, "Triethylamine gas sensor based on ZnO nanorods prepared by a simple solution route," *Sens. Actuators B* **141**(1), 85–88 (2009).
18. D. C. Olson, Y.-J. Lee, M. S. White, N. Kopidakis, S. E. Shaheen, D. S. Ginley, J. A. Voigt, and J. W. P. Hsu, "Effect of polymer processing on the performance of poly(3-hexylthiophene)/ZnO nanorod photovoltaic devices," *J. Phys. Chem. C* **111**(44), 16640–16645 (2007).
19. K. M. Coakley and M. D. McGehee, "Conjugated polymer photovoltaic cells," *Chem. Mater.* **16**(23), 4533–4542 (2004).
20. S. Peulon and D. Lincot, "Mechanistic study of cathodic electrodeposition of zinc oxide and zinc hydroxychloride films from oxygenated aqueous zinc chloride solutions," *J. Electrochem. Soc.* **145**(3), 864–874 (1998).
21. T. Yoshida, D. Komatsu, N. Shimokawa, and H. Minoura, "Mechanism of cathodic electrodeposition of zinc oxide thin films from aqueous zinc nitrate baths," *Thin Solid Films* **451**, 166–169 (2004).
22. K. M. Coakley and M. D. McGehee, "Photovoltaic cells made from conjugated polymers infiltrated into mesoporous titania," *Appl. Phys. Lett.* **83**(16), 3380–3382 (2003).
23. Y. Sun, G. M. Fuge, and M. N. R. Ashfold, "Growth of aligned ZnO nanorod arrays by catalyst-free pulsed laser deposition methods," *Chem. Phys. Lett.* **396**(1–3), 21–26 (2004).
24. M. N. R. Ashfold, R. P. Doherty, N. G. Ndifor-Angwafor, D. J. Riley, and Y. Sun, "The kinetics of the hydrothermal growth of ZnO nanostructures," *Thin Solid Films* **515**(24), 8679–8683 (2007).
25. L. E. Greene, M. Law, D. H. Tan, M. Montano, J. Goldberger, G. Somorjai, and P. Yang, "General route to vertical ZnO nanowire arrays using textured ZnO seeds," *Nano Lett.* **5**(7), 1231–1236 (2005).
26. J. Song and S. Lim, "Effect of seed layer on the growth of ZnO nanorods," *J. Phys. Chem. C* **111**(2), 596–600 (2006).

27. M. Guo, P. Diao, and S. Cai, "Hydrothermal growth of well-aligned ZnO nanorod arrays: Dependence of morphology and alignment ordering upon preparing conditions," *J. Solid State Chem.* **178**(6), 1864–1873 (2005).
28. M. Ohyama, H. Kouzuka, and T. Yoko, "Sol-gel preparation of ZnO films with extremely preferred orientation along (002) plane from zinc acetate solution," *Thin Solid Films* **306**(1), 78–85 (1997).
29. D. Boyle, K. Govender, and P. O'Brien, "Novel low temperature solution deposition of perpendicularly orientated rods of ZnO: Substrate effects and evidence of the importance of counter-ions in the control of crystallite growth," *Chem. Commun.* **2002**, 80–81 (2002).
30. L. Vayssieres, "Growth of arrayed nanorods and nanowires of ZnO from aqueous solutions," *Adv. Mater.* **15**(5), 464–466 (2003).
31. B. N. Illy, B. Ingham, and M. P. Ryan, "The effect of the supersaturation on the growth of zinc oxide nanostructured films by electrochemical deposition," *Crys. Growth Des.* **10**, 1189–1193 (2010).
32. C.-T. Hsieh, S.-Y. Yang, and J.-Y. Lin, "Electrochemical deposition and superhydrophobic behavior of ZnO nanorod arrays," *Thin Solid Films* **518**(17), 4884–4889 (2010).
33. X. Zhu, Z. Zhang, X. Men, J. Yang, and X. Xu, "Fabrication of an intelligent superhydrophobic surface based on ZnO nanorod arrays with switchable adhesion property," *Appl. Surf. Sci.* **256**(24), 7619–7622 (2010).

Biographies and photographs of the authors not available.